engineering proceedings

MDPI

Proceeding Paper

Structural Comparison of Raw Sodium Bicarbonate and Hydrated Lime for Dry SO_2 Removal †

Robert Makomere [1,*], Lawrence Koech [2], Hilary Rutto [1], Alfayo Alugongo [3], Sammy Kiambi [1] and Ngeleshi Kibambe [4]

[1] Clean Technology and Applied Materials Research Group, Department of Chemical and Metallurgical Engineering, Vaal University of Technology, Private Bag X021, Vanderbijlpark 1900, South Africa; hilaryr@vut.ac.za (H.R.); sammyk@vut.ac.za (S.K.)
[2] Department of Chemical, Metallurgical and Materials Engineering, Tshwane University of Technology, Pretoria, Private Bag X680, Pretoria 0001, South Africa; koechlk@tut.ac.za
[3] Department of Industrial Engineering, Operation Management, and Mechanical Engineering, Vaal University of Technology, Andries Potgieter Blvd, Private Bag X021, Vanderbijlpark 1911, South Africa; alfayoa@vut.ac.za
[4] Center for Nanoengineering and Advanced Materials (CeNAM), School of Mining, Metallurgy, and Chemical Engineering, University of Johannesburg, Doorfontein Campus, Johannesburg 2028, South Africa; ngeleshik@gmail.com
* Correspondence: 220178178@edu.vut.ac.za; Tel.: +27-(0)-16-950-6742
† Presented at the 3rd International Electronic Conference on Processes—Green and Sustainable Process Engineering and Process Systems Engineering (ECP 2024), 29–31 May 2024; Available online: https://sciforum.net/event/ECP2024.

Abstract: In dry flue gas treatment systems, gas–solid interactions are modulated by the reagent molecular composition and physical attributes. In the present investigation, sodium- and calcium-based sorbents were screened for structural and compositional variations for their subsequent application in sulphur dioxide capture. Mined sodium bicarbonate ($NaHCO_3$) in its unprocessed form and commercial-grade hydrated lime ($Ca(OH)_2$) were subjected to morphological analyses, employing scanning electron microscopy (SEM), particle size distribution (PSD), Brunauer–Emmett–Teller surface area evaluation, and Barrett–Joyner–Halenda (BJH) pore structure classification. Fourier Transform Infrared Spectroscopy (FTIR) was leveraged for a surface elemental chemical assessment. Pursuant to the BET report, $Ca(OH)_2$ presented a larger specific surface area (4.2360 m^2/g) as opposed to $NaHCO_3$ (0.2303 m^2/g), which was supported by the weighted mean value (D43) from the PSD analysis. Although $Ca(OH)_2$ had a higher pore volume (0.089822 cm^3/g), the totality of the $NaHCO_3$ pore size (117.312 Å) was classified as mesoporous. The SEM assessment suggested that the lower $NaHCO_3$ surface area stemmed from larger particle sizes. The FTIR spectrum indicated a greater carbonate concentration in the $NaHCO_3$ sorbent material, which also structures the pore morphology of the reagent. These findings offer critical information pertinent to the intricate dry flue gas desulphurisation process. The data generated will help us to design fixed bed experiments in a subsequent study.

Keywords: calcium hydroxide; emission mitigation; sodium bicarbonate; sulphation; sorbent screening

check for updates

Citation: Makomere, R.; Koech, L.; Rutto, H.; Alugongo, A.; Kiambi, S.; Kibambe, N. Structural Comparison of Raw Sodium Bicarbonate and Hydrated Lime for Dry SO_2 Removal. *Eng. Proc.* **2024**, *67*, 63. https://doi.org/10.3390/engproc2024067063

Academic Editor: Juan Francisco García Martín

Published: 10 October 2024

Copyright: © 2024 by the authors. Licensee MDPI, Basel, Switzerland. This article is an open access article distributed under the terms and conditions of the Creative Commons Attribution (CC BY) license (https://creativecommons.org/licenses/by/4.0/).

1. Introduction

The availability of highly reactive and cost-effective sorbents for dry flue gas desulphurisation (DFGD) creates a conundrum for process designers. Unlike wet and semi-dry systems that use slurry reagents, the sulphation activity in the DFGD occurs between a powdered sorbent and the target sulphur dioxide (SO_2) gas [1]. In hindsight, maximal SO_2 capture profits from an ideal gas–solid interaction, which is influenced by the sorbent reaction area and pore morphology. Hydrated lime ($Ca(OH)_2$) is primarily preferred in dry systems due to its high reactivity and finer particle sizes that induce a higher surface area

compared to limestone ($CaCO_3$) and lime (CaO) [2]. Unrefined sodium-based sorbents can serve as standard reagent compounds with a higher reactivity than Ca^{2+}, Equation (1), as suggested by the increased reactivity of Na^+, Equation (2), in the reactivity series.

The sulphation process benefits from the interaction with a strong basic $Ca(OH)_2$ salt (pH ≈ 12.4) as the reaction kinetics with an acidic gas are faster. This chemistry enables the maintenance of pH levels during the neutralisation process, thereby enhancing reaction performance. Sodium bicarbonate (pH ≈ 8.3) displays amphoteric properties and can be applied as an alkali reagent in sulphation reactions. Despite being a weak base, several investigators have indicated high SO_2 removal efficiencies with sodium-based sorbents [2–4].

$$Ca(OH)_{2(s)} + H_2O_{(l)} \rightleftharpoons Ca^{2+}_{(aq)} + OH^-_{(aq)} : pH \approx 12.4 \text{ @ } 25\ ^\circ C \quad (1)$$

$$NaHCO_{3(s)} + H_2O_{(l)} \rightleftharpoons Na^+_{(aq)} + OH^-_{(aq)} + H_2CO_{3(aq)} : pH \approx 8.3 \text{ @ } 25\ ^\circ C \quad (2)$$

Gas–solid intimate contact in DFGD is directed by the ability of the flue gas to effectively diffuse into desulphuriser particles, initiate a surface chemical reaction, and diffuse through the product layer to the unreacted surface. As a result, particle size affects the surface area and the availability of active sites after product layer formation. Generally, the molar volume of the product (sulphite–SO_3^{2-} and sulphate–SO_4^{2-}) formed after SO_2 capture is larger than the unreacted particle, which reduces the accessible reaction area [5].

In this paper, $Ca(OH)_2$ and $NaHCO_3$ will be subject to scanning electron microscopy (SEM), Brunauer–Emmett–Teller (BET), Barrett–Joyner–Halenda (BJH), particle size distribution (PSD), and ex situ Fourier Transform Infrared Spectroscopy (FTIR) analysis to study the surface properties and functional groups concerning SO_2 adsorption. Emphasis will be based on particle size, pore distribution, and pore density. $Ca(OH)_2$ can be generated through a reaction of lime (CaO) and water in a hydration procedure, which further upsurges operational costs, particularly in retrofit applications. In contrast, nahcolite is a naturally occurring mineral salt consisting of $NaHCO_3$ that necessitates no formulation processes for desulphurisation. Therefore, it is vital to simultaneously analyse the structural and chemical characteristics of these two sorbents, offering significant insights into the elements influencing their reactivity during SO_2 extraction and establishing the basis for enhancing DFGD procedures.

2. Materials and Methods

Sodium bicarbonate in its natural form (nahcolite) was sourced from Botswana Ash (Pty) Ltd. (Botash), Alrode, South Africa. From the energy dispersive systems (EDSs) analysis, $NaHCO_3$ was found to have a mineralogical composition of 98.47% Na_2O, 1.38% P_2O_5, 0.01% CaO, 0.06% TiO_2, and 0.07% MnO. Hydrated lime was of commercial grade (86.9 wt. %) from Kayla Africa, Wadeville, South Africa. It had a mineral species of 90.18% CaO, 0.23% Na_2O, 1.12% MgO, 0.79% Al_2O_3, 7.43% SiO_2, 0.13% SO_3, 0.05% K_2O, 0.06% TiO_2, 0.12% MnO_4, 0.19% SrO, and 0.02% ZrO_2.

Nitrogen adsorption–desorption appraised the specific surface area (SSA), pore volume, and pore size using the BET and BJH procedures in a micromeritics analyser. SEM assessments employed a Philips XL-30S machine, while the Malvern Mastersizer 2000 conducted sorbent PSD measurements within the 0.01–2000 μm limit. The PerkinElmer Spectrum Two FTIR device characterised the surface functional groups of the sorbents in the 4500 to 500 cm^{-1} wavenumber range.

3. Results and Discussion

Subject to N_2 adsorption–desorption (77 K), Table 1 revealed that $Ca(OH)_2$ had a higher reaction surface (4.2360 m^2/g) for SO_2 scrubbing compared to $NaHCO_3$ (0.2303 m^2/g). Ideally, a sorbent with a larger exposed surface promotes optimum gas–solid interaction, which is required for a successful sulphation reaction in a dry FGD system [6]. $Ca(OH)_2$ had a pore size of 601.753 Å (60.1753 nm), classified in the macro pore size range (>50 nm)

and a volume of 0.089822 cm^3/g. $NaHCO_3$ displayed mesopore (2–50 nm) pore sizes of 117.312 Å (11.7312 nm), falling within the ideal region of SO_2 capture. In comparison to $Ca(OH)_2$, the $NaHCO_3$ pore volume was lower, at 0.000639 cm^3/g [7,8].

Table 1. Physical properties of $Ca(OH)_2$ and $NaHCO_3$ from BET and BJH analysis.

Physical Property	$Ca(OH)_2$	$NaHCO_3$
BET surface area, m^2/g	4.2360	0.2303
BET pore size, Å	601.753	117.312
BJH pore volume, cm^3/g	0.089822	0.000639
* HK maximum pore volume, cm^3/g	0.003861	0.000705

* Horvath–Kawazoe report on maximum pore volume analysed at relative pressures (P/Po) of 3.0022×10^{-9} for $Ca(OH)_2$ and 3.02357×10^{-9} for $NaHCO_3$.

The SEM observations complemented the BET results by revealing a larger $NaHCO_3$ particle size (Figure 1c) as opposed to $Ca(OH)_2$ (Figure 1d), viewed at the same scale of 1 µm. The orientation of the $NaHCO_3$ directly impacted the available reaction area for efficient sulphation reaction. Conventionally, larger particle sizes exhibit lower SA, as seen in Table 1. From Figure 1a, $NaHCO_3$ is characterised by intraparticle pores, which are beneficial for SO_2 diffusion and likely stem from the cohesion of irregularly shaped particles (lumps) during material conception [9]. This supplements the pore morphology on the $NaHCO_3$ particle surface, evident in Figure 1c. The $Ca(OH)_2$ structure appears to have a spherical shape and is also formed from the aggregation of smaller independent particles (Figure 1b,d). The uneven clumping of individual particles during hydration results in a void formation [10], although not as pronounced as in $NaHCO_3$. The resulting higher HK maximum pore volume of 0.003861 cm^3/g for $Ca(OH)_2$ suggests a microporous pore diameter. Generally, SO_2 capture is promoted by a reagent having mesoporous properties as it limits diffusion resistances, compared to the smaller micropores. From this, even though $Ca(OH)_2$ exhibits a higher surface area, raw $NaHCO_3$ can be considered a similarly competitive adsorbent from the dense surface and intraparticle pore existence.

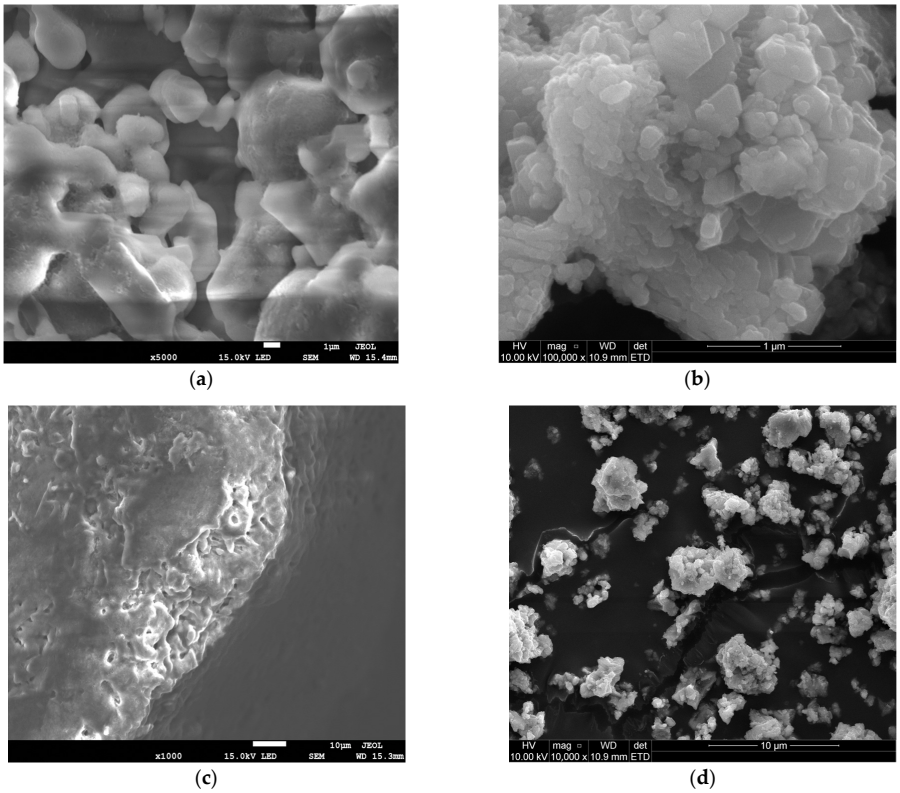

(**a**) (**b**) (**c**) (**d**)

Figure 1. SEM images of $NaHCO_3$ sorbent—(**a**,**c**) and $Ca(OH)_2$ sorbent—(**b**,**d**).

Particle size determines the exposure of active sites to the target acidic gas. Desirable sorbent particles should be small and refined to attain a greater surface area. Figure 2a provides the PSD data for both reagents, indicating a multimodal distribution with various particle size ranges. The mean volume diameter of the smallest particle range is nearly identical, with $Ca(OH)_2$ at 5.77 µm and $NaHCO_3$ at 5.67 µm. However, the nahcolite salt ($NaHCO_3$) includes coarse particles ranging from 100 to 1000 µm. The coarse particle fraction of calcium hydroxide ranges from 10 to 100 m. $Ca(OH)_2$ exhibits a considerably lower weighted mean value (D43) of 47.58 µm as opposed to nahcolite, which has a D43 of 130.833 µm, confirming finer particle orientation. The cumulative distribution plot in Figure 2b illustrates this finding.

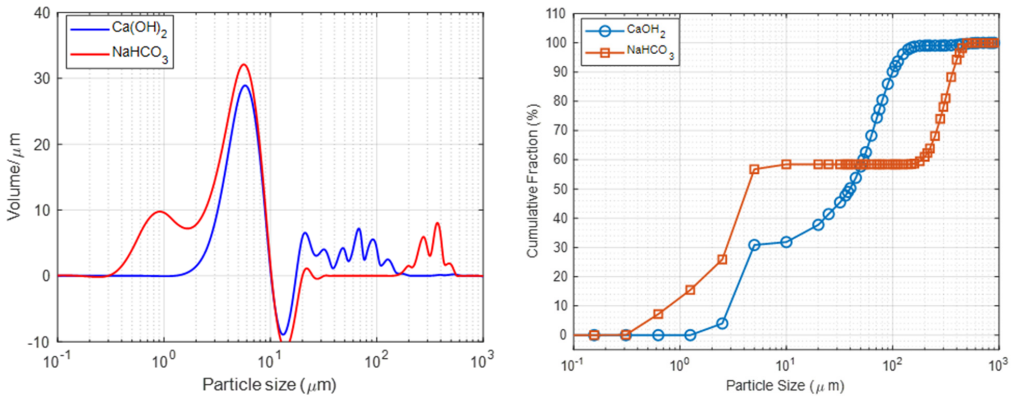

(**a**) (**b**)

Figure 2. (**a**) Particle size distribution and (**b**) reagent cumulative distribution of the $Ca(OH)_2$ and $NaHCO_3$.

Understanding the chemical bonds necessary for sorbent activity is useful in examining the molecular structural differences between $Ca(OH)_2$ and $NaHCO_3$. The reaction temperature in the DFGD units surpasses 120 °C, ensuring the breakdown of $NaHCO_3$ to Na_2CO_3 (Equations (3) and (4)) as the active species (popcorn effect), contrary to $Ca(OH)_2$ (Equation (5)) which reacts in its native form [11]. The sulphation byproduct generated mainly comprises a dry sulphite salt. The ex situ FTIR spectrum from Figure 3a displays the sharp hydroxyl stretching band (O–H) at 3643 cm^{-1} responsible for the strong alkaline property (pH ≈ 12.4), suggesting a hexagonal h-CaO phase. Calcite ($CaCO_3$) formation at 2522 cm^{-1} corresponds to a reaction with free CO_2 whose eventuality reduces the active $Ca(OH)_2$ sites, considering the poor $CaCO_3$ activity in dry FGD. The broad peak at 1427 cm^{-1} depicts the irregular stretching of CO_3^{2-}. The O–C–O in-plane bending peak vibrations are marked at 713 cm^{-1}, while the v_2 out-of-plane bending is centered at 875 cm^{-1} [12]. The nahcolite structure in Figure 3b illustrates a higher carbonate concentration at 1427 cm^{-1} (CO_3^{2-} group), 875 cm^{-1} (CO_2 out-of-plane bending), and 702 cm^{-1} (O–C–O bending vibrations). The peaks at 1773 cm^{-1} and 597 cm^{-1} relate to HCO_3^- and OC–(OH), respectively. The formation of the weak carbonic acid (H_2CO_3) and its interaction with the hydroxyl group (OH) results in the reduced alkalinity of the $NaHCO_3$ sorbent [13]. This feature influences the reactivity of the acid–base sulphation process. As a strong base, $Ca(OH)_2$ has a higher ability to accept protons in a reaction with a strong acid, ensuring that the reaction process is completed and a stable product is formed. $NaHCO_3$, however, falls second in the reactivity series and hence possesses a greater tendency to engage in a reaction. The contrast presented by the physiochemical properties of these reagents is the motivation to pursue a direct sorbent injection process simulating dry FGD. Both sorbents will be tested for dry SO_2 removal, where additional data concerning the reaction mechanisms,

spontaneity, and molecular interactions between the gas and the adsorbent will be studied and compared.

$$NaHCO_{3(s)} \overset{\Delta H \geq 120^{\circ}C}{\rightarrow} Na_2CO_{3(s)} + H_2O_{(g)} + CO_{2(g)} \quad (3)$$

$$Na_2CO_{3(s)} + SO_{2(g)} \rightarrow Na_2SO_{3(s)} + CO_{2(g)} \quad (4)$$

$$Ca(OH)_{2(s)} + SO_{2(g)} \rightarrow CaSO_{3(s)} + H_2O_{(g)} \quad (5)$$

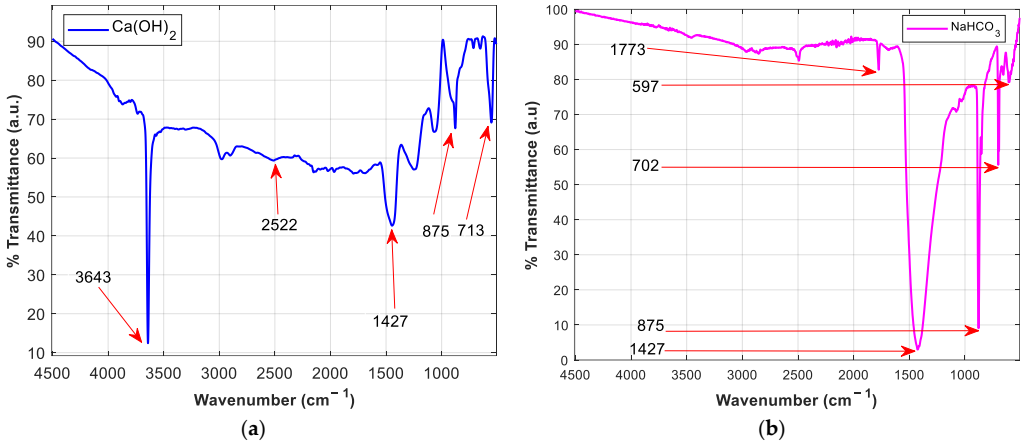

Figure 3. FTIR spectrum of (**a**) $Ca(OH)_2$ and (**b**) $NaHCO_3$ (nahcolite).

4. Conclusions

The screening assessments within this paper were aimed at evaluating the chemical and physical attributes of the $Ca(OH)_2$ and $NaHCO_3$ reagents relevant to dry desulphurisation. It should be noted that $NaHCO_3$ was considered in its raw form (nahcolite) as an alternative, given the higher cost price associated with $Ca(OH)_2$ synthesis techniques. Both sorbents have alkaline properties and can attract acidic SO_2 gas in flue gas. Available reaction sites processed by BET and BJH report show $Ca(OH)_2$ would promote more gas–solid contact given the superior SSA of 4.2360 m^2/g and pore volume (BJH) of 0.089822 m^2/g. $Ca(OH)_2$ had smaller and finer particles as per the SEM micrographs and PSD calculations, attaining a volume mean diameter (D43) of 47.58 µm. Upon chemical reaction, this sorbent possesses performance advantages. Nonetheless, SO_2 diffusion through the $NaHCO_3$ particles was stimulated by its mesoporous property of 11.7312 nm, aside from the larger and coarser particles indicated by a D43 of 130.83 µm. Additionally, the internal pores observed in the SEM analysis validated $NaHCO_3$ integration in the sulphation process. Molecular characterisation from the FTIR outcome indicated that the combination of CO_3^{2-} and HCO_3^{-} formed a more significant proportion of the surface chemical groups, from which the hydrogen potential of $NaHCO_3$ was 8.3. Additionally, this involved an interaction with the OH group in the $NaHCO_3$ structure, reducing the basicity. The more significant proportion of the hydroxyl band (OH) in the $Ca(OH)_2$ sorbent outweighed the contaminant $CO3^{2-}$ groups; hence, the basic reactivity was scarcely affected. While $Ca(OH)_2$ has beneficial properties based on the characterisation reports, raw $NaHCO_3$ cannot be disregarded as a prospective substitute for DFGD as well as an alternative to what is obtained from the Solvay process.

Author Contributions: Conceptualisation, R.M. and L.K.; methodology, R.M., L.K., H.R., A.A. and S.K.; formal analysis, R.M., L.K, H.R., A.A. and N.K.; investigation, R.M. and L.K.; resources, L.K., H.R., A.A. and N.K.; data curation, R.M. and L.K.; writing—original draft preparation, R.M.; writing—review and editing, R.M., L.K., H.R., A.A. and S.K.; visualisation, R.M. and L.K.; supervision, L.K., H.R. and A.A.; project administration, L.K., H.R. and A.A. All authors have read and agreed to the published version of the manuscript.

Funding: This research received no external funding.

Institutional Review Board Statement: Not applicable.

Informed Consent Statement: Not applicable.

Data Availability Statement: The data presented in this study are available on request from the corresponding author.

Acknowledgments: The authors acknowledge Ngeleshi Kibambe for invaluable assistance with the scanning electron microscopy (SEM) analysis, which greatly contributed to the quality of this research.

Conflicts of Interest: The authors declare no conflicts of interest.

References

1. Deng, Y.; Ansart, R.; Baeyens, J.; Zhang, H. Flue Gas Desulphurization in Circulating Fluidised Beds. *Energies* **2019**, *12*, 3908. [CrossRef]
2. Carpenter, A.M. *Low Water FGD Technologies*; IEA Clean Coal Centre: London, UK, 2012; Vol December 2012.
3. Walawska, B.; Szymanek, A.; Pajdak, A.; Nowak, M. Flue Gas Desulfurization by Mechanically and Thermally Activated Sodium Bicarbonate. *Pol. J. Chem. Technol.* **2014**, *16*, 56–62. [CrossRef]
4. Omidi Bibalani, I.; Ale Ebrahim, H. Kinetic Study of Low-Temperature Sulfur Dioxide Removal Reaction by Sodium Carbonate Using Random Pore Model. *Environ. Sci. Pollut. Res.* **2022**, *29*, 6334–6346. [CrossRef] [PubMed]
5. Makomere, R.S.; Rutto, H.L.; Koech, L. The Use of Cellulose Nanocrystals to Support $Ca(OH)_2$ Nanoparticles with Diatomite Incorporation in Sulphur Capture at Low Temperatures: Optimisation and Modelling. *Arab. J. Sci. Eng.* **2023**, *48*, 8871–8885. [CrossRef]
6. Maina, P.; Mbarawa, M. Enhancement of Lime Reactivity by Addition of Diatomite. *Fuel Process. Technol.* **2011**, *92*, 1910–1919. [CrossRef]
7. Wang, K.-Q.; Gao, X.-M.; Lin, B.; Hua, D.-X.; Yan, Y.; Zhao, H.-Y.; Xiao, W.-D. An Efficient Calcium-Based Sorbent for Flue Gas Dry-Desulfurization: Promotion Roles of Nitrogen Oxide and Oxygen. *RSC Adv.* **2023**, *13*, 1312–1319. [CrossRef] [PubMed]
8. Koech, L.; Everson, R.; Neomagus, H.; Rutto, H. Dissolution Kinetics of South African Coal Fly Ash and the Development of a Semi-Empirical Model to Predict Dissolution. *Chem. Ind. Chem. Eng. Q.* **2015**, *21*, 319–330. [CrossRef]
9. Sudibyo, S.; Suharto, S.; Rarasati, S.A.A.; Wulandari, Y.R.; Shintawati, S.; Rohman, F.S. Optimization of Sodium Bicarbonate Production from Ammonium Hydroxide Using a Froth Flotation Column. *Chem. Eng. Technol.* **2022**, *45*, 1952–1959. [CrossRef]
10. Dong, Y.; Zhang, M.; Xie, C. Effect of Reaction Conditions on Agglomeration of Aluminum Hydroxide in the Recovery of Waste Aluminum-Catalyst. *Sep. Purif. Technol.* **2020**, *248*, 116978. [CrossRef]
11. Mchabe, D.; Hattingh, B.B.; Koech, L.; Rutto, H.; Neomagus, H.W.J.P. Sodium-Based Flue Gas Desulphurisation for the South African Coal-Fired Power Industry a Review. *S. Afr. J. Chem. Eng.* **2024**, *48*, 167–183. [CrossRef]
12. Samanta, A.; Chanda, D.K.; Das, P.S.; Ghosh, J.; Mukhopadhyay, A.K.; Dey, A. Synthesis of Nano Calcium Hydroxide in Aqueous Medium. *J. Am. Ceram. Soc.* **2016**, *99*, 787–795. [CrossRef]
13. Engelking, L.R. Chapter 93—Alkalinizing and Acidifying Solutions. In *Textbook of Veterinary Physiological Chemistry*, 3rd ed.; Engelking, L.R., Ed.; Academic Press: Boston, MA, USA, 2015; pp. 606–611, ISBN 978-0-12-391909-0.

Disclaimer/Publisher's Note: The statements, opinions and data contained in all publications are solely those of the individual author(s) and contributor(s) and not of MDPI and/or the editor(s). MDPI and/or the editor(s) disclaim responsibility for any injury to people or property resulting from any ideas, methods, instructions or products referred to in the content.